horticulturae

MDPI

Article

Physiological and Molecular Studies on the Chitosan-N Confers Anti-PRSV Ability of *Carica Papaya* L.

Jinhui Lv [1,2], Na An [2], Yvqing Guan [1,2] and Ping Chen [1,2,*]

[1] School of Breeding and Multiplication (Sanya Institute of Breeding and Multiplication), Hainan University, Sanya 572025, China; lvjinhuixue@163.com (J.L.); guanyuqing01@163.com (Y.G.)
[2] Key Laboratory for Quality Regulation of Tropical Horticultural Crops of Hainan Province, School of Tropical Agriculture and Forestry, Hainan University, Danzhou 571737, China; xysanna225@163.com
* Correspondence: chenping08213@163.com

Abstract

Prevention and control of papaya ringspot virus (PRSV) is a difficult problem for papaya growers all over the world. CTS-N (Chitosan-N) can alleviate viral pathogenesis by inducing defense-related enzymatic activities. In this study, we quantified superoxide anion production, assayed the activities of defense enzymes (POD, PPO, SOD, and chitinase), and measured the contents of key phytohormones (ETH, JA, SA, and ABA). Based on transcriptomic data from our preliminary work, the full-length *CpRBOHD* gene was cloned using RACE (Rapid amplification of cDNA ends). A plant overexpression vector was subsequently constructed and agroinfiltrated into PRSV-infected papaya leaves. Expression dynamics of *CpRBOHD* were analyzed by qPCR, and concomitant changes in physiological indices were evaluated. The application of 1.0 g/L CTS-N significantly enhanced defense enzyme activities and elevated phytohormone levels. The coding sequence (CDS) of the *CpRBOHD* gene was 2760bp. Transient overexpression of *CpRBOHD* in PRSV-infected leaves resulted in a marked upregulation of its expression, as confirmed by qPCR. This was accompanied by increased activities of SOD, CAT, and PAL, alongside a reduction in MDA content. These findings indicate that increased *CpRBOHD* expression is associated with enhanced resistance to PRSV. The identification of PRSV-responsive genes represents a promising strategy for breeding resistant cultivars. Collectively, our results provide a theoretical basis for the biological control of papaya ringspot disease.

Keywords: papaya; CTS-N; PRSV; defense enzymes; *CpRBOHD* gene

Academic Editor: Ángel Emilio Martínez De Alba

Received: 29 August 2026
Revised: 22 October 2026
Accepted: 30 October 2026
Published: 3 November 2026

Copyright: © 2026 by the authors. Licensee MDPI, Basel, Switzerland. This article is an open access article distributed under the terms and conditions of the Creative Commons Attribution (CC BY) license.

1. Introduction

Papaya (*Carica papaya* L.) is one of the unique herbal fruit trees in tropical and subtropical areas. The World Health Organization ranked it top among ten fruits with the most nutritional value [1]. In recent years, one of the most serious diseases in the papaya-related planting and cultivation industry at home and abroad has been the papaya ringspot virus (PRSV) disease caused by the genus Potyvirus [2]. In the early stages of PRSV, water-stained circular spots appear on the surface of the leaves. The longer the time of infection with PRSV, the more ringspots will form, which will show mosaic symptoms. In severe cases, the leaves will become like chicken feet, making it difficult for them to develop into normal leaves [3,4]. When the damage to papaya plants is more extensive, growth vigor declines, and fruit production decreases. When the disease is severe, it

causes the death of all papaya plants cultivated in large fields [5]. The mutation of the virus is rapid in Hainan, and regional and environmental climate changes have also reduced the resistance of transgenic papayas [3]; therefore, it is particularly important to find a method that can confer broad-spectrum resistance to control this viral disease.

CTS-N not only increases photosynthesis and promotes and enhances plant growth but also induces innate immune responses in plants. In the field of agriculture, the scope of its application is also wide, and it can regulate the increase in plant yield and harvest [6]. Its main component is chitosan (CTS), which is a kind of cationic polysaccharide. It is also an eco-friendly biopesticide that enhances the innate ability of plants to resist fungal infections [7]. Chitosan can be obtained from crustacean shells. Zhang et al. investigated the control of papaya ringspot virus (PRSV) disease using three inducers (chitosan, salicylic acid, and jasmonic acid). They found that all three inducers exhibited some efficacy; however, pure chitosan showed relatively poorer performance, with a control efficacy of approximately 20% [8]. In contrast, Zhang et al. reported that among three biopesticides, CTS-N was the most effective against papaya virus disease, with the compound formulation CTS-N achieving a control efficacy of approximately 70% [2]. Moreover, owing to its good film-forming properties, it is widely used as a seed coating. Liu et al. studied corn seed and seedlings treated with chitosan in combination with Cu, Mn, Fe, and Zn, and showed that it significantly reduced salt stress and improved the salt tolerance of seedlings [9,10].

The determination of defense enzyme activity has been widely used to evaluate stress resistance in plants. Plants maintain low ROS levels by producing various secondary metabolites and defense enzymes. Common defense enzymes include superoxide dismutase (SOD), peroxidase (POD), and polyphenol oxidase (PPO) [7]. Chitosan can scavenge free radicals and protect DNA from damage [11]. Some studies have shown that chitinase is a defensive enzyme. In addition, certain plant hormones regulate chitinase activity. Studies have shown that ethylene (ETH), jasmonic acid (JA), salicylic acid (SA), and abscisic acid (ABA) are all associated with the enzyme chitinase [12]. Therefore, the degree of plant oxidation can be determined by measuring the activity of defense enzymes, and the relationship between hormones and plant stress resistance can be explained by determining the concentration of plant hormones.

By introducing PRSV-resistant genes, papaya plants can be made resistant to PRSV. Kumar et al. [13] cultivated papaya transformed with CP and GFP fusion genes to improve the ability of transgenic papaya strains to resist PRSV infection, based on sequence homology analysis of transgenic sources. Jia et al. [14] cultivated CP-transgenic papaya-related strains, which have some research and application value against PRSV. Genetic engineering can be used as a better way to prevent and control papaya disease inbreeding, which makes it possible for plants to resist PRSV, improve the breeding effect, and shorten the breeding time.

Respiratory burst oxidase homolog (RBOH) is also known as nicotinamide adenine dinucleotide phosphate oxidase (NOX) [15]. Plant RBOH family proteins are composed of a conserved domain that combines NADPH and FAD, two heme unit domains, and six transmembrane helix domains. The plant RBOH protein contains Ca^{2+} bound EF-hand treatments at the N-terminus [16]. The expression of the *RBOH* gene in plants is the main source of reactive oxygen species (ROS). Research on ROS-related effects mainly shows that the plant itself induces a hypersensitive response (HR) when it interacts with non-affinity pathogens [17]. Studies in recent years have shown that reactive oxygen species can induce plants to produce substances that inhibit the infection of pathogens, as well as simultaneously inducing defensive responses of plants in signaling pathways [18]. Respiratory burst oxidase homologues (RBOHs) in plants are the enzymes responsible for producing $O_2^{\bullet -}$ via flavin-containing NADPH oxidases localized at the plasma membrane

[19]. The roles of RBOH-derived $O_2^{\bullet-}$ in AR formation have been elucidated in many plant species, such as mung bean [20], cucumber [21], Arabidopsis [22], poplar [23], and apple [24]. Therefore, NADPH oxidase in plants is the main source of ROS generated when germs and plants interact, and is considered to be one of the necessary conditions for ROS outbreak. NADPH oxidase thus plays an important role in regulating ROS production during plant resistance to biological stress.

In this study, PRSV morphology was observed in papaya leaves, and the optimal concentration of CTS-N was determined. The activities of four defense enzymes (SOD, POD, PPO, and chitinase) and the content of four plant hormones (ETH, JA, SA, and ABA) were measured in papaya to describe the changes in plant immunity after applying CTS-N. Currently, there is a lack of information on the molecular mechanisms of papaya anti-PRSV, and there are few reports on the successful cloning and identification of papaya anti-PRSV-related genes. In this study, using the transcriptome data of "Transcriptome of Papaya Anti-PRSV Virus-Induced by CTS-N (Chitosan-N)" obtained from the preliminary test of the subject [25], a gene that was significantly upregulated during anti-PRSV was cloned by rapid amplification of cDNA ends (RACE) to obtain its full length, and then bioinformatics-related analysis, gene expression analysis, and anti-PRSV effect were verified on the sequence. Using papaya anti-PRSV gene resources to understand how the papaya gene controls PRSV, we laid a foundation for screening and cultivating papaya germplasm with stable PRSV control and biological safety. The results of this study provide a new idea for future research on PRSV control, as well as new strategies for controlling plant viruses in other plants.

2. Materials and Methods

2.1. Materials

The experiment was conducted in the greenhouse of the Hainan University Experimental Base. The materials used were "Tainong No.2" papaya seedlings. (This species of papaya has been commercialized and is not a rare plant. It does not require any permission to be used as a sample.) The seeds were obtained from the Lihe Seedlings Company (Taiwan, China). The PRSV was obtained from the Institute of Biotechnology, Chinese Academy of Tropical Agricultural Sciences. PRSV needs to be preserved on the living leaves of papaya plants.

GV3101 (*Agrobacterium tumefaciens*), *Escherichia coli* DH5a, and *Rosetta* (DE3) were purchased from Weide Biotechnology Co., Ltd. (Shanghai, China). The PCXSN (35S promoter, Kanamycin, Hygromycin, 10,802 bp) and Pet28a-sumo (T7 promoter, Kanamycin, 5629 bp) plasmids were purchased from Yitian Biotechnology Co., Ltd. (Hainan, China). He jiaan (bottled) was purchased from Saniodine Biochemical Co., Ltd. (Shandong, China). The main components of CTS-N (He jiaan) are as follows: chitosan ≥ 20 g/L, organic matter ≥ 100 g/L, total nitrogen ≥ 60 g/L, water-insoluble matter ≤ 50 g/L, chloride ions ≤ 30 g/L, and pH 5.0–8.5.

2.2. Methods

2.2.1. Cultivation and Treatment of Papayas

This experiment was conducted as a pot experiment in an open-field environment. Prior to the experiment, routine fertilization and water management were applied. At the time of seedling transplantation, the basal substrate for the pots was prepared by thoroughly mixing nutrient soil and vermiculite at a 1:1 ratio (*v*/*v*). The flower pots used had a diameter of 32 cm and a height of 35 cm. During the experimental period, plants were fertilized once every three days. The height of the plants was approximately 40 cm. There were 10 seedlings in each treatment. Three sets of repetitions were performed for each

treatment, and each trial was conducted independently and repeatedly. Each repetition had 3–4 seedlings. Mixed samples were collected from the leaves of different plants within the same replicate. The experiment was a single-factor field experiment with a negative control and a positive control. The variable applied was the concentration of CTS-N. Different concentrations of CTS-N were applied to the flower pots on day 0 of the experiment. The three concentrations of CTS-N were 0.5 g/L (Treatment A), 1 g/L (Treatment B), and 1.5 g/L (Treatment C). The five treatments were marked as CK−, CK+, A, B, and C; in Treatments CK− and CK+, CTS-N concentrations were replaced with the same volume of fresh water. Treatment CK− only included clear water, whereas Treatment CK+ was inoculated with PRSV. One day later, four treatment groups (CK+, A, B, and C) were simultaneously inoculated with papaya ringspot virus (PRSV). Subsequently, all five treatment groups were irrigated and fertilized normally for cultivation. Physiological indicators were measured on the day of CTS-N application (0 d), as well as at 24 h (1 d), 4 d, 6 d, 13 d, and 21 d post-application. For each treatment, the second and third fully expanded functional leaves, counting from the leaf heart (apical meristem), were collected from papaya seedlings to measure the aforementioned indicators. Each treatment was performed with three biological replicates. The virus inoculation method adopted was tissue fluid friction inoculation. We first ground 1 g of virus-infected leaves into a fine powder using liquid nitrogen. Then, 100 mL of phosphate buffer (pH 7.8) was added, and the mixture was further ground into a homogenate. The homogenate was filtered to remove residues and immediately used for inoculation (1.5 mL/plant). We dipped a small amount of tissue fluid and quartz sand with the thumb and index finger, and rubbed it gently on the surface of the papaya leaf to create a small wound on the surface of the leaf. After CTS-N was applied, enzyme activity and phytohormone content were determined. PRSV was inoculated only once at the beginning.

Leaves (1 g) were ground with 9 mL of pH 7.8 buffer and centrifuged at 12,000 rpm for 10 min. The precipitate was discarded, and the supernatant was extracted. This was repeated twice. The crude enzyme solution was then used for physiological tests. The crude enzyme solution was diluted according to the experimental requirements during various determinations. Each treatment was performed in triplicate. The morbidity of all papayas was observed on the 0th, 12th, 17th, 22nd, and 27th days after inoculation with PRSV. The incidence rate was calculated as the percentage of diseased plants in the total number of plants in each treatment. Papaya is considered pathogenic when its leaves appear as spots or curls. The formula is as follows:

Plant incidence (per treatment) = Number of symptomatic plants/Total plants × 100%

2.2.2. PRSV Identification Method

In order to determine whether the samples were infected with the virus, the blade slurry of the samples was observed by transmission electron microscopy, referring to the test method of Chen [26]. The specimen preparation methods are shown in the Supporting Information File. RNA extraction was performed according to the instructions provided with the RNAprep Pure Plant Kit (DP432; Tiangen Biotechnology Co., Ltd., Beijing, China); see Figure S4 RNA identification gel image. Reverse transcription was performed using the TransScript® one-step gDNA Removal and cDNA Synthesis SuperMix kit (AT311, TransGen Biotechnology Co., Ltd. Beijing, China). The main reaction system is shown in Table S2. It was incubated at 25 °C for 10 min, then at 42 °C for 30 min, followed by incubation at 85 °C for 5 s, and finally cooled to 4 °C for long-term storage at a constant temperature. After that, it can be taken out for use and temporarily frozen at −20 °C. At the same time, at the molecular level, PRSV was identified by RT-PCR and qPCR. Primers were designed according to the PRSV (Accession No: EF183499) conserved region, and

the primers were PRSV-1F and PRSV-1R (Table S1) [3]. The PCR amplification system (Table S3) was preheated at 94 °C for 3 min, into the cycle step for 35 times with denaturation at 94 °C for 30 s, annealing at 55 °C for 20 s, extension at 72 °C for 1 min, and final extension at 72 °C for 10 min, then saved at 4 °C. The qPCR reaction was performed using the ChamQ Universal SYBR qPCR Master Mix (Q711-02, Vazyme Biotechnology Co., Ltd., Nanjing, China) reagent and cDNA, referring to the article by Tuo et al.; we selected *Carica papaya* actin-7 (LOC110816158, XM_088222843.1) as the reference gene for qPCR validation [3]. The Ct values of Actin in all samples were analyzed, and the coefficient of variation (CV) was 0.3%. its amplification efficiency was 95%, and the melting curve was unimodal. The primers used in the qPCR reaction were Actin-F, Actin-R, PRSV-F, and PRSV-R (Table S1). In the qPCR amplification system (Table S4), the amplification reaction was initiated with an initial denaturation at 95 °C for 10 min, followed by 45 cycles of a three-step protocol: denaturation at 95 °C for 30 s, annealing at 55–65 °C for 30 s, and extension at 72 °C for 30 s to 1 min. Fluorescence signals were collected at the end of the annealing step at 55 °C. Subsequently, melting curve analysis was performed, which consisted of an initial denaturation at 95 °C for 30 s, followed by continuous fluorescence acquisition during a gradual temperature increase from 55 °C to 95 °C.

2.2.3. Determination of Physiological Indicators

The total superoxide dismutase (T-SOD) test kit (A001-1, Jiancheng Bioengineering Institute, Nanjing, China) was used, and SOD activity was measured using the nitroblue tetrazolium (NBT) method with slight modifications according to Wang et al. [27]. Detailed experimental procedures can be found in the Supporting Information File. Unit definition: One unit (U) of SOD activity was defined as the amount of enzyme required to inhibit the photoreduction of NBT by 50% in 1 mL of reaction mixture per gram of tissue. The peroxidase (POD) test kit (A084-3, Nanjing Jiancheng Bioengineering Institute, China) was used, and POD activity was measured using the guaiacol colorimetric method [28]. Detailed experimental procedures can be found in the Supporting Information File. Unit definition: One unit (U) of POD activity was defined as the amount of enzyme that catalyzes the conversion of 1 μg of substrate per minute per gram of tissue at 37 °C. The polyphenol oxidase (PPO) test kit (A136-1-1, Nanjing Jiancheng Bioengineering Institute, China) was used; PPO catalyzes phenolic substrates to produce quinones, which exhibit characteristic absorbance at 420 nm. The activity of PPO was measured according to the method of Li and Gong [29] with slight modifications. Detailed experimental procedures can be found in the Supplementary Material. Unit definition: One unit (U) of PPO activity was defined as the amount of enzyme that causes an increase in absorbance at 420 nm of 0.01 per minute per gram of tissue in 1 mL of reaction mixture.

Chitinases were determined using a double-antibody sandwich enzyme-linked immunosorbent assay (ELISA) with a microplate reader; they were measured using an ELISA kit (Kete Company, Jiangsu, China). Detailed steps can be found in the Supporting Information File. All other reagents used were of analytical grade. Chitinase activity was determined using an ELISA kit produced by Kete Company (Jiangsu, China). The content of superoxide anions was determined using the hydroxylamine hydrochloride azo reaction colorimetric method, according to Li and Gong [30]. The superoxide anion radical ($O_2^{\bullet -}$) reacts with hydroxylamine hydrochloride to form nitrite (NO_2^-). Under acidic conditions, the generated nitrite undergoes a diazotization reaction with sulfanilic acid and subsequently couples with α-naphthylamine (or N-1-naphthylethylenediamine dihydrochloride) to form a pink azo dye. This product exhibits a maximum absorption peak at 530 nm. The amount of nitrite generated was calculated based on a $NaNO_2$ standard curve (Supporting Information File) and then converted to superoxide anion production. Ethylene (ETH), jasmonic acid (JA), abscisic acid (ABA), and salicylic acid (SA) levels in plants

were measured using double-antibody sandwich ELISA kit (Kete Company, Jiangsu, China); the standard curve and detailed steps can be found in the Supporting Information File.

2.2.4. RACE Cloning of CpRBOHD Gene

The corresponding sequences of *CpRBOHD* (NCBI: XM_022044550) were obtained by referring to the annotation information of CTS-N anti-PRSV transcriptome data from a previous study. Primer 5.0 software was used for primer design. The primers were GSP (RBOHD-5 'RACE/RBOHD-3' RACE), T0, and T1 (Table S1). RACE cloning was performed using the SMARTer RACE5 '/3' Kit (Cat.Nos.634859, TaKaRa Biotechnology Co., Ltd. Beijing, China).

Using cDNA generated as a template for PCR amplification, the primers for cloning the intermediate sequence were RBOHD-F and RBOHD-R (Table S1). The reaction experimental conditions (Table S3) were as follows: preheating at 96 °C, denaturation at 96 °C for 30 s, annealing at 58 °C for 20 s, extension at 72 °C for 50 s for 35 cycles, and final extension at 72 °C for 3 min and 16 °C for 1 min. The target gene fragments amplified by PCR were detected by agarose gel electrophoresis. Cloning was performed by PCR amplification and gel electrophoresis; following figure observations, the corresponding target bands were cut and then purified using the pMD ™ 19—T Vector Cloning Kit (TaKaRa Biotechnology Co., Ltd. Beijing, China). The segments were inserted into a cloning vector and then into competent *Escherichia coli* DH5a cells; after shaking the bacteria overnight, monoclonal strains of bacterial liquid cultures were picked and the strains of positive clones were further identified before sending the results to a sequencing company for validation.

2.2.5. CpRBOHD Gene Bioinformatics Analysis

The online software used for *CpRBOHD* gene sequence-related bioinformatics prediction is shown in Table S5. Using DNAMAN 9.0 software of *CPRBOHD* gene encoding proteins in protein homology, *CpRBOHD* coding related proteins in the NCBI Blast database: https://blast.ncbi.nlm.nih.gov/Blast.cgi (accessed on 4 May 2026) with *Durio zibethinus* (XM-022917015.1), *Gossypium arboreum* (XM-017789470.1), and *Gossypium raimondii* (XM-012592906.1). The encoded protein was compared using MEGA 10 software, the comparison of the phylogenetic tree was completed according to the construction principle of the proximity method, and the main parameters were set as follows: distance model, p-distance; robustness test, bootstrap method, 1800 repetitions; processing of vacancy deletion data, pairwise deletion.

2.2.6. qPCR Detection of Genes in Samples

PRSV infection in papaya leaves was detected by RT-PCR in the early stages of the experiment, and PRSV was identified using morphological, cytological, and molecular biology methods. Papaya plants without PRSV infection (CK−) were used as the control treatment; treatments with PRSV infection and disease (CK+) and 1.0 g/L CTS-N irrigation and PRSV of infection and disease (B) The measurement experiment was carried out the fourth day. For the specific operation of qPCR, please refer to 2.2.2. The primers used in the qPCR reaction were Actin-F, Actin-R, PRSV-F, PRSV-R, qRboh-F, and qRboh-R (Table S1).

2.2.7. Prokaryotic Expression of CpRBOHD Gene

Prokaryotic expression primers were designed according to the confirmed CDS regions of the Y-*CpRBOHD* gene (Table S1). The bands in the CDS region of the Y-*CpRBOHD* gene were amplified by PCR, which was based on the cloning method of the intermediate

sequence in 2.2.2. Target fragments were purified using the Universal DNA Purification Kit (DP214, Tiangen Biotechnology Co., Ltd. Beijing China) and then reacted at 37 °C for 5 h using the method of double enzyme digestion (*BamHI* and *XhoI*). The prokaryotic expression plasmid pET28a-sumo and target DNA bands were cut. After cutting the reaction product, electrophoresis was performed, and the target bands were purified. The purified DNA target gene and open-chain linear vector pET28a-sumo were ligated using T4 DNA Ligase at 16 °C overnight. The pET28a-*CpRBOHD*-sumo recombinant plasmid was then transformed into the expression strain *Rosetta* (DE3).

Transformed strains containing the target *CpRBOHD* gene were inoculated into 150 mL LB liquid medium (supplemented with 50 μg/mL kanamycin). The medium was shaken until the OD600 = 0.6, and then IPTG (1 mmol/L) was added to the LB liquid medium containing the target gene and transformed strain to induce protein expression at 16 °C overnight. The sample (1 mL) was centrifuged at 1200 rpm for 2 min, and the precipitate was retained. Then, 100 μL of 1SDS-PAGE Loading Buffer was added to the precipitate and boiled at approximately 100 °C for 10 min, followed by cooling to room temperature. After centrifugation at 1200 rpm for 2 min, 10 μL of the upper layer liquid was collected, and the protein expression effect was verified using SDS-PAGE protein electrophoresis gel. Coomassie Brilliant Blue was used to stain the gel and observe the position of the protein bands.

2.2.8. Construction of CpRBOHD Gene Plant Overexpression Vector

The designed target gene primers are *CpRBOHD*-F and *CpRBOHD*-R (Table S1), Primer 5.0 software was used for primer design. The CDS zone bands of the *CpRBOHD* gene were amplified by PCR. Two endonucleases, *BsrGI* and *SalI*, were used to react at 37 °C for 4 h, and the pCXSN plasmid was cut into a linearized carrier. The overexpression vector of plants was constructed by homologous recombination, in accordance with the Gibson Cloning and Assembly Kit (CAT#:160680-20). After overnight culture, the corresponding monoclones were selected for PCR identification. Some bacterial solutions of the positive clones were sent to the company for base sequence sequencing. The remaining bacterial solution was stored at −80 °C for the next experiment. pCXSN-*CpRBOHD* reconstructed the overexpression vector and transferred it to the expressed strain GV3101.

2.2.9. Transient Expression of CpRBOHD Gene of Papaya Leaves Which Were Infected

Papaya seedlings were cultivated in the same environment, and plants were infected with PRSV when they had approximately 8 leaves. After 16 days of cultivation, ringspot symptoms were observed on the leaf surface. Subsequently, the leaves were infiltrated with Agrobacterium tumefaciens strain GV3101 carrying the *CpRBOHD* gene to achieve transient expression (culture conditions: supplemented with rifampicin 20 μg/mL, 50 μg/mL kanamycin, 28 °C, 18 h, OD = 0.8). Four treatments of papaya plants (3 plants in each treatment) were treated by injection. For each plant, the third fully expanded functional leaf counted from the apical meristem was selected for infiltration. Three infiltration sites were injected per leaf. A total of 1.5 mL of the infectious solution was injected into each leaf. Each treatment group consisted of three biological replicates, with each individual plant serving as one independent biological replicate. After 10 days of cultivation, the samples were collected for subsequent experiments. The treatments were as follows: plants that were not infected with PRSV and reconstructed overexpression vector were set as the negative control treatment (CK−); those infected with PRSV but not infected with reconstructed overexpression vector were set as the positive control treatment (CK+); those infected with PRSV and empty pCXSN vector were set as the control treatment (KZ); those infected with PRSV and reconstructed overexpression vector pCXSN-*CpRBOHD* were set as the RB treatment. Four treatments were cultured with proper watering and

fertilization. Four treatments were cultured for 10 days in the same environment for qPCR analysis of transient expression and assaying of related resistance physiological indices. Fully expanded functional leaves infected with Agrobacterium from papaya plants in each treatment were chosen to assay each index 3 times in duplicate tests.

The T-SOD test kit (A001-1) and catalase (CAT) test kit (A007-1-1, Nanjing Jiancheng Bioengineering Institute, China) were used. CAT activity was measured using the ammonium molybdate colorimetric method. The change in absorbance was monitored at 405 nm, and CAT activity was subsequently calculated. Detailed experimental procedures can be found in the Supporting Information File. Unit definition: One unit (U) of CAT activity was defined as the amount of enzyme that decomposes 1 μmol of H_2O_2 per second per gram of tissue. The phenylalanine ammonia lyase (PAL) test kit (A137-1-1, Nanjing Jiancheng Bioengineering Institute, China) was used. The PAL assay is based on its catalysis of L-phenylalanine to trans-cinnamic acid and ammonia. Trans-cinnamic acid exhibits a maximum absorption at 290 nm, and PAL activity is calculated by measuring the change in absorbance at this wavelength. Unit definition: One unit (U) of PAL activity was defined as the amount of enzyme that causes an increase in absorbance at 290 nm of 0.1 per minute per gram of tissue in 1 mL of reaction mixture. For the determination of malondialdehyde (MDA) content in plants, the experimental method of Tang et al. was referenced and optimized [28]. The principle is that under acidic conditions, heating thiobarbituric acid (TBA) reacts with MDA in papaya leaves to produce a colored reaction, yielding a reddish-brown substance (trimethine, 3,5,5-trimethyl-2,4-oxazolidinedione). Absorbance values are measured at 450 nm, 532 nm, and 600 nm, respectively, to calculate the MDA content. Detailed procedures can be found in the Supporting Information File. The MDA content can be used to evaluate the degree of cell damage and the intensity of plant stress resistance responses [31].

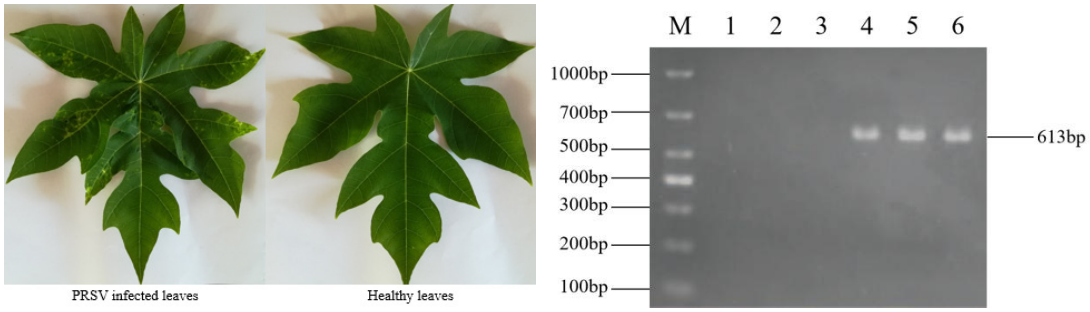
2.3. Data Processing

Data were processed using Microsoft Excel 2016. Comparisons among treatments were performed by two-way analysis of variance (two-way ANOVA), a least significant difference (LSD) multiple-comparison test, and Duncan's test using IBM SPSS 22. *T*-test analysis was conducted on the data ($p < 0.05$). We conducted a TOPSIS (Technique for Order of Preference by Similarity to Ideal Solution) analysis based on the principle of measuring the distance between two schemes using the Euclidean distance, by utilizing multiple physiological indicators that we had measured. This process was accomplished through Software SAS 9.0. analysis to calculate the ideal optimal solution. DNAMAN software was used for base sequence splicing (contig assembly). qPCR analysis was performed using the $2^{-\Delta\Delta Ct}$ method. Graphs were generated by means of GraphPad Prism 8.0.2. Each treatment consisted of three biological replicates. The error bars in the figure represent the standard deviation.

3. Results

3.1. Virus Detection Results of PRSV

After 16 days of PRSV inoculation, rings appeared on the leaves of the plants (Figure 1A), and the results of RT-PCR detection are shown in Figure 1B. The leaves that were not infected had no PRSV gene bands in lanes 1, 2, and 3, while gene bands of the infected leaves were clearly visible in lanes 4, 5, and 6.



(**A**) (**B**)

Figure 1. Leaf phenotypic and molecular identification of PRSV. Note: (**A**). Papaya diseased leaves infected with PRSV. (**B**). RT-PCR identification of PRSV content in papaya; lanes 1, 2, and 3 were plants without PRSV infection; lanes 4, 5, and 6 were plants with PRSV infection.

Figure 2 shows that PRSV in diseased leaves is a linear virus with a length of approximately 200–800 nm, which is a potato Y virus. These observations are similar to those of Liu et al. [32] and Sun et al. [33]. Figure 2(1,2) show the virus particles in the CK+ treatment and electron microscopy images of two negative stains in the CK+ treatment. One particle is observed in Figure 2(1), and the other is in Figure 2(2). Treatment B also resulted in two negative stains, but no viruses were found. Therefore, there are no more photos to show here. Moreover, no virus particles were observed in Treatment B, probably because of the low virus content.

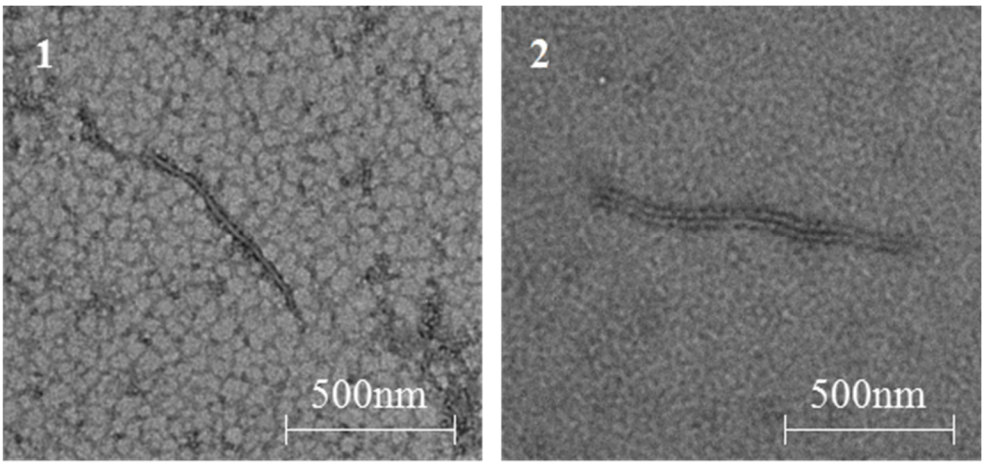


Figure 2. Transmission electron microscopy observation of PRSV. Note: Figure 2(**1**) has only one complete virus particle; 2(**2**) has two complete virus particles. The scale is 1 cm: 500 nm.

3.2. Effect of CTS-N on Morbidity of Papaya

As shown in Figure 3, except for the non-inoculated CK− treatment, all other treatments inoculated with PRSV showed varying degrees of morbidity, and the overall morbidity rate slowly increased. The morbidity of papaya in the CK+ treatment was always higher than that in the three experimental treatments (A, B, and C), and in the CK+ treatment, it continued to increase significantly in subsequent days. In the experimental treatment, due to the application of CTS-N, although there was some morbidity, it was lower than that in the CK+ treatment. Simultaneously, by laterally comparing Treatments A, B, and C, we observed that the morbidity of papaya in C was generally higher than that of A and B, and the increase rate was also relatively higher. Furthermore, the morbidity of papaya in Treatment C on the 17th and 22nd days was the same as that of the CK+ treatment. Therefore, we can infer that the application of CTS-N may have some influence on the morbidity of papaya plants. The concentration of CTS-N within a certain range has a

positive effect on the disease resistance of papaya, whereas a high concentration reduces this positive impact and can even have a negative impact.

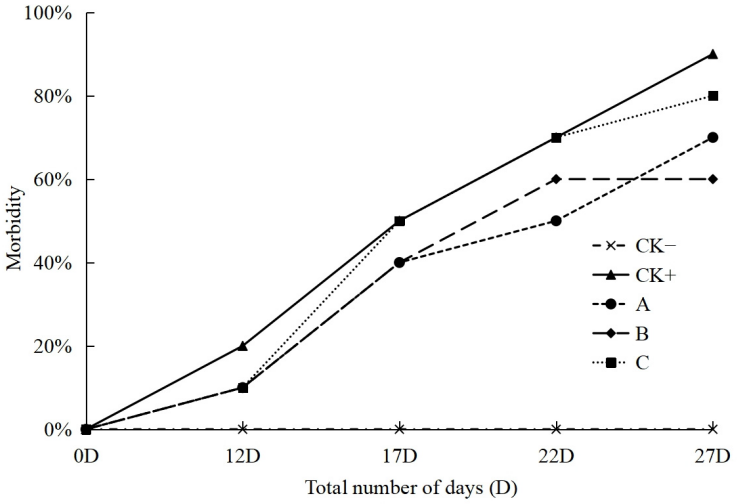


Figure 3. Changes in the morbidity of papaya with time. Note: CK− stands for negative control (clear water irrigation only); CK+ stands for positive control (PRSV inoculation only); A stands for treatment with 0.5 g/L CTS-N solution irrigation and PRSV inoculation; B stands for treatment with 1 g/L CTS-N solution irrigation and PRSV inoculation; C stands for treatment with 1.5 g/L CTSN solution irrigation and PRSV inoculation.

3.3. Effect of Stress-Resistance-Related Enzyme Activity

PPO can catalyze phenol and oxyradicals, reduce or prevent infection, and thus improve disease resistance. The trend of PPO activity is shown in Figure 4A. On the first day of CTS-N application, PPO activity began to increase. On the fourth day after applying CTS-N (the first day after inoculation with PRSV), it can be seen that the PPO activity of Treatment B reached a peak. The activity of PPO in the three treatments (A, B, and C) was also close to the peak and began to decline on the thirteenth day. Treatment B was more tolerant of stress than the other treatments in the PPO assay. Overall, the PPO activity of the three treatments was higher than that of CK+, and the change trend was relatively small. POD catalyzes an oxidation reaction that is related to the outbreak of reactive oxygen. The POD activity in Treatments A, B, and C increased significantly. The disease was relatively mild at that time. The POD activity in the three treatments was always at a high level, whereas that in CK− and CK+ was lower. The results show that the stress resistance of the experimental treatments was higher than that of the control. According to the data, the POD activity in Treatment B was significantly increased and showed the highest value (Figure 4B).

SOD can convert reactive oxygen species to hydrogen peroxide and oxygen, which are harmless to the cells when the plants are adversely affected, thereby protecting the cells infected by the pathogenic substances. Figure 4C shows that SOD activity in the post-administration CTS-N treatment rapidly increased, whereas it increased slowly in CK− and CK+. The changes in SOD activity in Treatments B and C were particularly significant. Chitinase plays an important role in plant disease resistance, and its content in plants rapidly increases after infection by pathogenic substances. As shown in Figure 4D, the chitinase activity in the CK− and B treatments showed a decreasing trend at first and then increased, while the other treatments showed an initial increase followed by a decrease. The CK+ treatment (control) showed a rapid rise from the first day after PRSV inoculation, which was the fourth day of the experiment, and reached a peak on the sixth day of the

experiment. In general, the peak values of chitinase in the three experimental treatments were much higher than those in the two control treatments without CTS-N. Through the comparative analysis of these three experimental treatments, we found that CTS-N treatment may require a certain reaction time to promote chitinase content in papaya virus strains ($p < 0.05$).

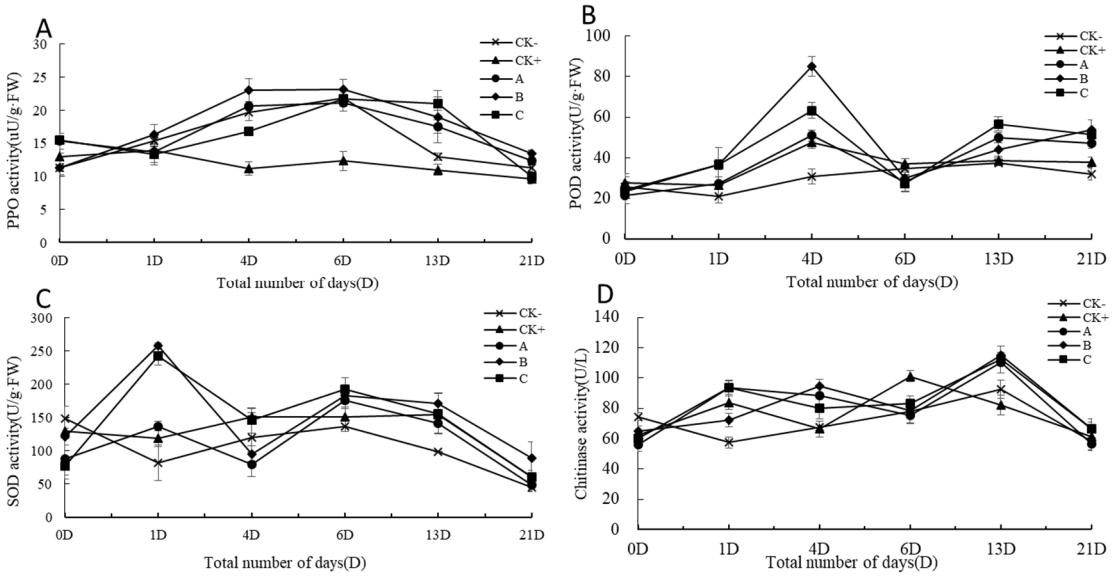


Figure 4. Changes in (**A**) PPO, (**B**) POD, (**C**) SOD, and (**D**) chitinase activities over time. Note: CK− stands for negative control (clear water irrigation only); CK+ stands for positive control (PRSV inoculation only); A stands for treatment with 0.5 g/L CTS-N solution irrigation and PRSV inoculation; B stands for treatment with 1 g/L CTS-N solution irrigation and PRSV inoculation; C stands for treatment with 1.5 g/L CTS-N solution irrigation and PRSV inoculation. The error bars indicate pooled standard errors of the means.

3.4. Effects of Related Hormones and the Content of Small Molecular Substances

As shown in Figure 5A, the ETH content in the experimental and control treatments was low before the application of CTS-N, whereas it increased after the application of CTS-N, except for CK−. After four days of inoculation, all the other treatments showed an upward trend, except for CK−. In particular, for Treatment B, the response to virus stress was rapid and reached its peak at the earliest. In the 13th and 21st day trials, the ETH content in Treatment B remained at the highest level, followed by Treatment A. In the end, the ETH content in the treatments was slightly higher than the initial content, and that in Treatment B was the highest, except for CK− and CK+, which almost recovered to the initial level.

JA and methyl jasmonate (MeJA) are widely deposited in plants as damage-related plant hormones and signaling molecules. As shown in Figure 5B, JA content was the highest in Treatment B and the lowest in the C and CK+ treatments before the application of CTS-N. After the application of CTS-N, except for B and CK−, the rest showed an upward trend. On the first day after inoculation, which was the fourth day of the test, the highest JA content was observed in Treatment B, followed by Treatment A, while that in B and the rest of the treatments showed significant differences ($p < 0.05$), and the JA level in the negative control CK− was the lowest. Additionally, it can be seen that Treatment B reached a peak value first, followed by the other treatments after three days; then, the levels of JA in all experimental treatments and the control showed a downward trend. On the last day of the experiment (21st day), the JA content dropped completely, but that of Treatment B remained the highest.

ABA is an endogenous plant hormone that plays a critical role in plant drought, high salt, low temperature, and other disease resistance. It is also known as the "stress hormone" [34]. According to Figure 5C, the change in ABA content was similar to that of JA content, especially in Treatment B. The ABA content of the experimental treatments and the control was almost at the same level before the application of CTS-N. However, after applying CTS-N, there was an increasing trend in all five treatments. On the first day of inoculation, which was the fourth day of the trial, the ABA content of Treatment B reached its peak value. Treatments C, CK−, and CK+ reached their peak value after 3 days of inoculation, i.e., on the 6th day of the trial. On the 13th day of the trial, the ABA level of each treatment reached a peak value and then showed a downward trend. Nevertheless, the ABA content of Treatments A, B, and C was significantly different from those of CK− and CK+ on the thirteenth day ($p < 0.05$).

SA and JA are hormone signaling substances that are closely associated with plant disease resistance. As shown in Figure 5D, the endogenous SA in papaya showed a general increasing trend, but the degree of increase was small. The SA content was stable during CTS-N application and was almost the same in all treatments. On the 4th day, Treatment B reached its peak value. However, the remaining treatments reached their peak values in subsequent days, with Treatment C reaching the highest value on the sixth day, while Treatment A reached the peak value on the thirteenth day of the trial. Subsequently, the SA level of papaya treated with CTS-N in Treatments A, B, and C began to decline on the thirteenth day, and CK+ was the final treatment to reach a peak ($p < 0.05$).

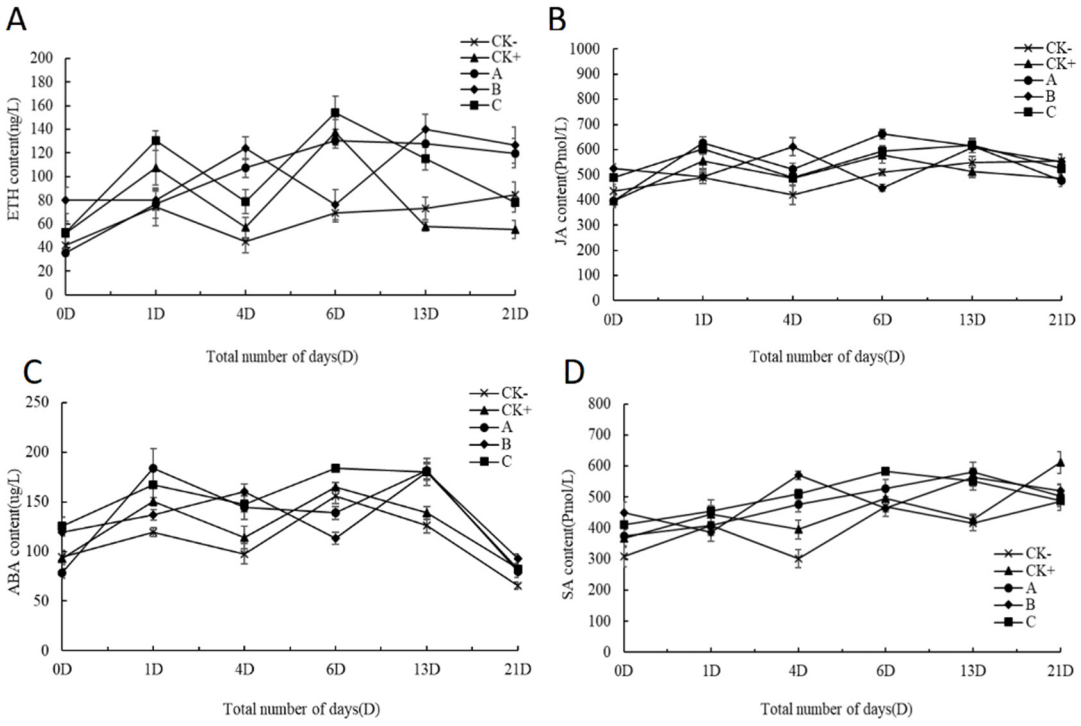


Figure 5. Changes in (**A**) ETH, (**B**) JA, (**C**) ABA, and (**D**) SA contents over time. Note: CK− stands for negative control (clear water irrigation only); CK+ stands for positive control (PRSV inoculation only); A stands for treatment with 0.5 g/L CTS-N solution irrigation and PRSV inoculation; B stands for treatment with 1 g/L CTS-N solution irrigation and PRSV inoculation; C stands for treatment with 1.5 g/L CTS-N solution irrigation and PRSV inoculation. The error bars indicate pooled standard errors of the means.

3.5. Changes in the Content of Superoxide Anion

Superoxide anions play a crucial role in environmental stress in plants, but the accumulation of oxyradicals is toxic to cells. According to Figure 6, there was little difference in the content of superoxide anion among all treatments in the first few days before the test. However, after PRSV inoculation, the content of superoxide anion among the A, C, and CK+ treatments increased significantly, but compared with CK+, the content of superoxide anion in A, B, and C was lower. Among them, the content of superoxide anion in Treatment B was almost always low. After inoculation, all treatments were affected and their content of superoxide anion increased significantly in all of them. The results of our study show that the content of superoxide anion in Treatment B almost always remained low, which indicates that the concentration of the plant immune regulator used in this treatment had the best effect on reducing the content of superoxide anion, suppressing the oxidizing ability. It may have prevented the structural and functional damage to the papaya plant.

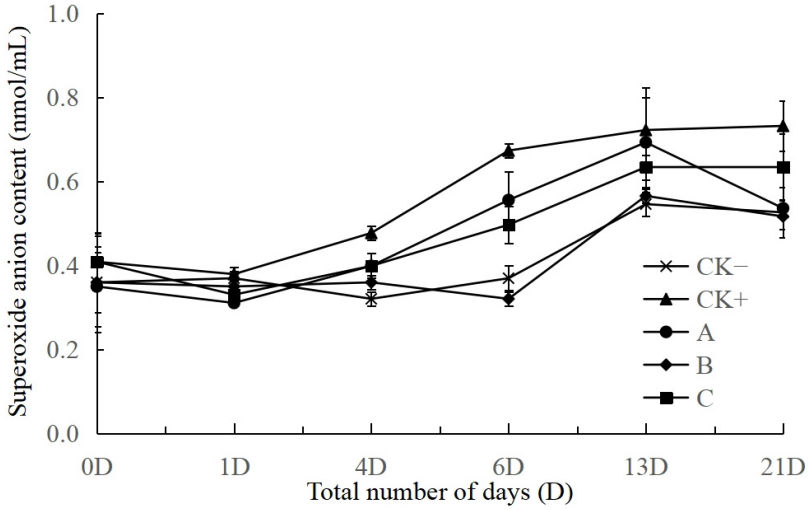


Figure 6. Changes in the content of superoxide anion. Note: CK− stands for negative control (clear water irrigation only); CK+ stands for positive control (PRSV inoculation only); A stands for treatment with 0.5 g/L CTS-N solution irrigation and PRSV inoculation; B stands for treatment with 1 g/L CTS-N solution irrigation and PRSV inoculation; C stands for treatment with 1.5 g/L CTS-N solution irrigation and PRSV inoculation. The error bars indicate pooled standard errors of the means.

3.6. TOPSIS Analysis

At 24 h post-virus inoculation, the enzyme activities of oxidoreductases exhibited a rapid increasing trend, and phytohormones also showed a similar trend at the same time point. After the determination of the above series of physiological indices, the values of all indicators in papaya treated with CTS-N at 24 h were higher than those at other times, and this can be regarded as an important turning point of the test. Table 1 presents the ranking results of the TOPSIS comprehensive analysis for all physiological indices on the 4th day of the experiment, which corresponds to 24 h post-virus inoculation. The processing of Treatment B ranked first, and those of A and C ranked second and third, respectively. The result conforms to the disease pattern of papaya. and Treatment B (1.0 g/L) was the most appropriate and effective concentration against PRSV.

Table 1. TOPSIS analysis.

Text	d_max	d_min	c	Order
CK−	0.6143	0.2131	0.2576	5
CK+	0.5462	0.1928	0.2609	4
A	0.2239	0.5031	0.692	2
B	0.0926	0.6704	0.8786	1
C	0.3627	0.381	0.5123	3

Note: CK− stands for negative control (clear water irrigation only); CK+ stands for positive control (PRSV inoculation only); A stands for treatment with 0.5 g/L CTS-N solution irrigation and PRSV inoculation; B stands for treatment with 1 g/L CTS-N solution irrigation and PRSV inoculation; C stands for treatment with 1.5 g/L CTS-N solution irrigation and PRSV inoculation.

3.7. Analysis of CpRBOHD Gene RACE Cloning Results

Based on transcriptomic data of *CpRBOHD* in papaya induced by CTS-N against PRSV obtained in the early stage of this project [25], the RACE cloning results of the *CpRBOHD* gene were as follows: the final sequenced 3′-RACE clone was 450 bp (Figure S1A), the 5′-RACE clone was 450 bp (Figure S1B), and the internal sequenced clone was 3516 bp (Figure S1C). The total length of the spliced full-length gene was 3905 bp. BLAST alignment in NCBI showed that the nucleotide sequence shared 100% identity with the reported *CpRBOHD* sequence in papaya, and the CDS of this gene was determined to be 2760 bp. The sequencing results were consistent with expectations, confirming that the RACE-amplified sequence corresponded to a known, existing transcript. Therefore, in this study, we obtained the full-length sequence of an already annotated transcript.

3.8. Predicting the Signal Peptides and Transmembrane Structures of CpRBOHD Gene Expression Proteins

The results showed that the CpRBOHD protein contained 20 amino acid types with a total of 919 residues. Leucine (Leu) was the most abundant amino acid (9.2%), while cysteine (Cys, 1.1%) and tryptophan (Trp, 2.1%) were the least abundant. The predicted molecular weight of the protein was 103.74 kDa, with a molecular formula of $C_{4675}H_{7292}N_{1268}O_{1329}S_{38}$. The theoretical isoelectric point (pI) was 9.25, indicating that the protein is alkaline. SignalP-4.1 online software was used to predict the location of signal peptide cleavage sites. The cleavage sites of the CpRBOHD signal peptide were determined based on the maximum Y-value, and the mean S-score was used to assess whether the protein is secreted. The results show a maximum Y-value of 0.031 and a mean S-score of 0.116, both below the predefined threshold. Therefore, the CpRBOHD protein is non-secretory and is not a signal peptide (Figure S2). TMHMM-2.0 and ProtTM were used to predict the transmembrane topology of the CpRBOHD protein online. The protein was identified as a transmembrane protein containing 6 alpha transmembrane helices: transmembrane domain 1 (371–390 aa), transmembrane domain 2 (409–429 aa), transmembrane domain 3 (453–472 aa), transmembrane domain 4 (510–531 aa), transmembrane domain 5 (555–574 aa), and transmembrane domain 6 (584–604 aa) (Figure S3). These results suggest that *CpRBOHD* may function as a membrane receptor involved in signal transduction. The amino acid sequences of the protein encoded by *CpRBOHD* were submitted to the NCBI database for BLASTp analysis. The sequence showed high identity with Rboh proteins from *Durio zibethinus* (78.52%), *Gossypium arboreum* (77.88%), and *Gossypium raimondii* (78.90%) (Figure 7). Phylogenetic analysis was performed using MEGA 10 with homologous protein sequences downloaded from NCBI (Figure 8). The phylogenetic tree showed that the *CpRBOHD* from papaya clustered into the same clade with orthologs from *D. zibethinus*, *G. arboreum*, and *G. raimondii* can converge into the same branch.

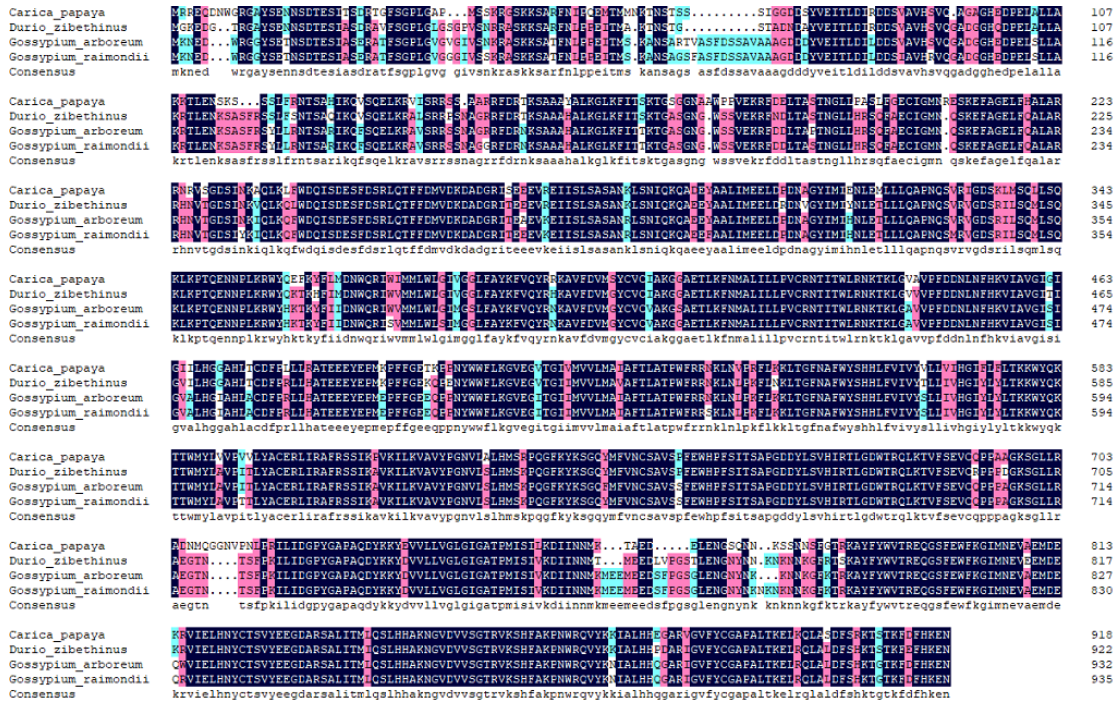


Figure 7. Alignments of amino acid sequences of *CpRBOHD* and similar proteins from other species.

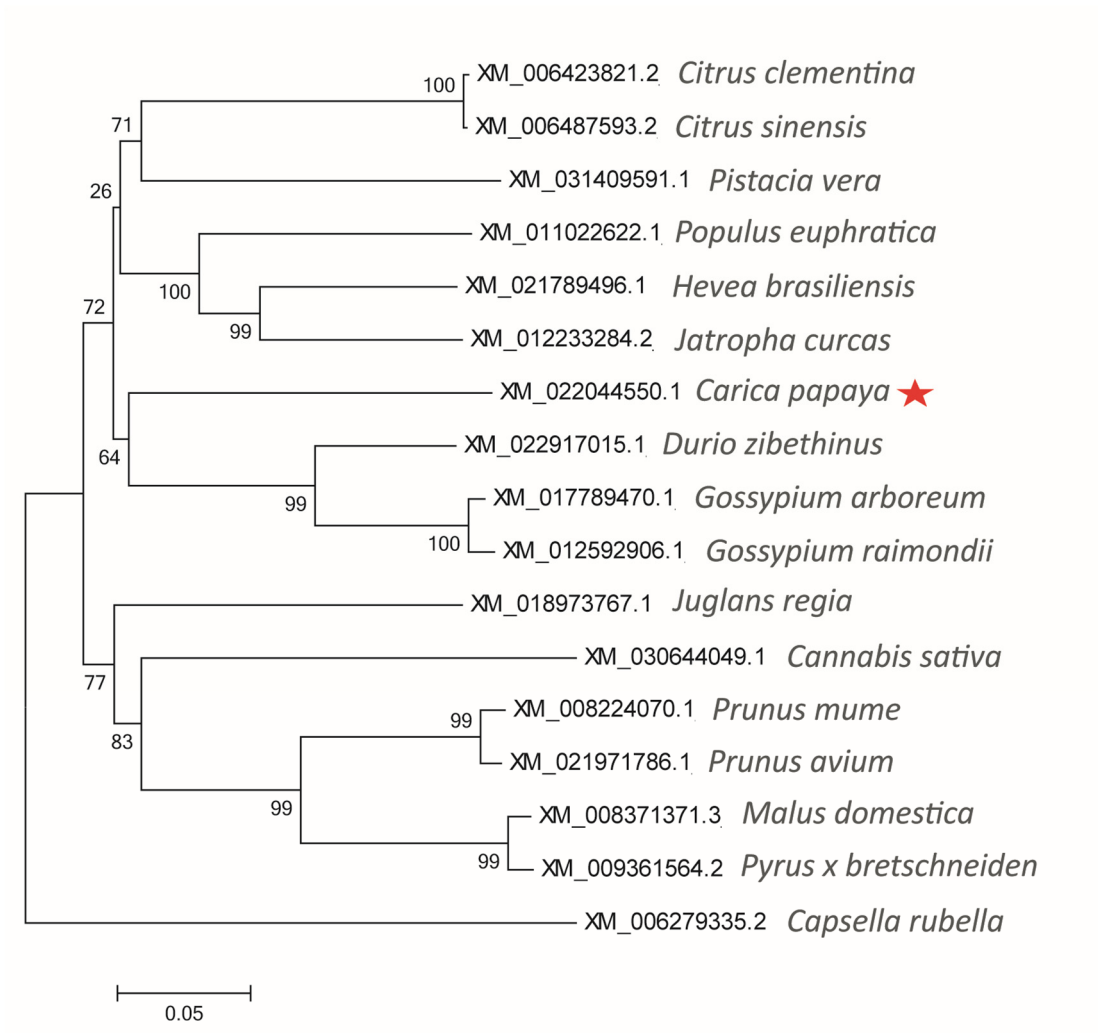
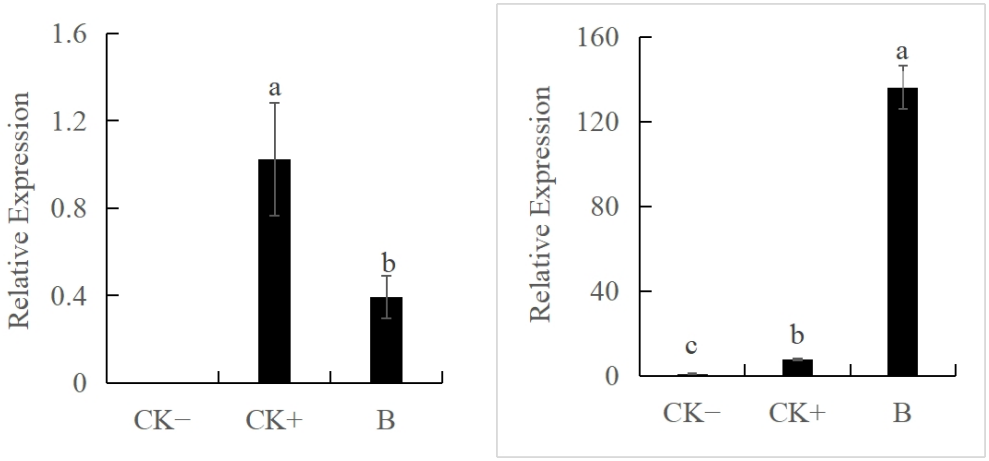


Figure 8. Phylogenetic tree of *CpRBOHD* protein.

3.9. qPCR Results of CpRBOHD Gene Expression in Samples

For the three different treatments of papaya leaf extracts, RNA was isolated (Figure S4), and then cDNA was reverse-transcribed. Subsequently, qPCR analysis was conducted. The relative expression levels of *PRSV* and *CpRBOHD* were analyzed by qPCR in papaya plants subjected to three treatments: CK−, CK+, and B. As shown in Figure 9A, the relative expression level of PRSV was ranked as CK+ (1.02) > B (0.39) > CK− (0). The expression level in Treatment B was approximately 2-fold lower than that in CK+ ($p < 0.05$), indicating a significant difference between treatments. As shown in Figure 9B, the relative expression level of *CpRBOHD* was ranked as B (136.19) > CK+ (7.66) > CK− (1.00). The expression level in Treatment B was significantly higher than those in CK+ and CK− ($p < 0.05$).



(**A**) (**B**)

Figure 9. Gene expression in different processed samples of papaya leaves. Note: (**A**) and (**B**) show the relative expression of PRSV and the *CpRBOHD* gene, respectively.

3.10. Prokaryotic Expression Analysis of CpRBOHD Gene

Bioinformatic prediction indicated that the *CpRBOHD* protein contains six transmembrane domains, which hinder the soluble expression of the full-length CDS in prokaryotic systems. Therefore, a highly hydrophilic fragment (2271–2760 bp, 489 bp in length) of the *CpRBOHD* CDS was selected for prokaryotic expression. The recombinant plasmid pET28a-*CpRBOHD*-sumo was constructed, verified by colony PCR (Figure S5), and confirmed by sequencing to contain the correct 489 bp insert. As shown in Figure 10, compared with the control (1), treatment (2) produced a distinct protein band between 14 kDa and 20 kDa, consistent with the theoretical molecular weight of 18.73 kDa for the truncated *CpRBOHD* fusion protein, confirming successful expression of the target protein.

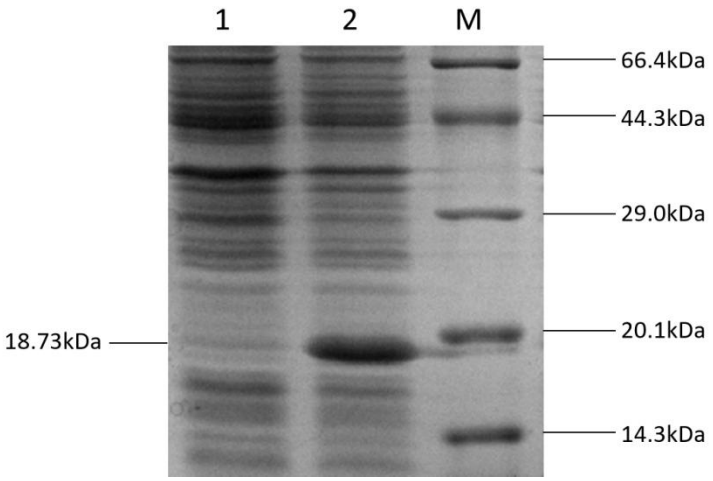


Figure 10. SDS-PAGE analysis of *CpRBOHD*. Note: M, protein marker; 1, control, no IPTG induction; 2, 1mmol/L IPTG induction.

3.11. Transient Expression of CpRBOHD Gene in Papaya Leaves Infected with PRSV

3.11.1. The CpRBOHD Gene Expression Was Verified by qPCR

Papaya leaves were agroinfiltrated for transient expression with either the reconstructed overexpression vector pCXSN-*CpRBOHD* (RB) or the empty vector pCXSN (CK+). As shown in Figure 11A, the relative expression level of PRSV was ranked as CK+ (2.66) > KZ (2.51) > RB (1.33) > CK− (0). Compared with CK+, the PRSV expression level in the RB treatment was reduced by more than 50% ($p < 0.05$). *CpRBOHD* showed significant differences among the three treatments. The relative expression levels of *CpRBOHD* across treatments are shown in Figure 11B, with the ranking RB (9.04) > CK+ (3.5) > KZ (1.13) > CK− (0.73). The expression level of *CpRBOHD* in the RB treatment was more than twice as high as that in the CK+ treatment ($p < 0.05$).

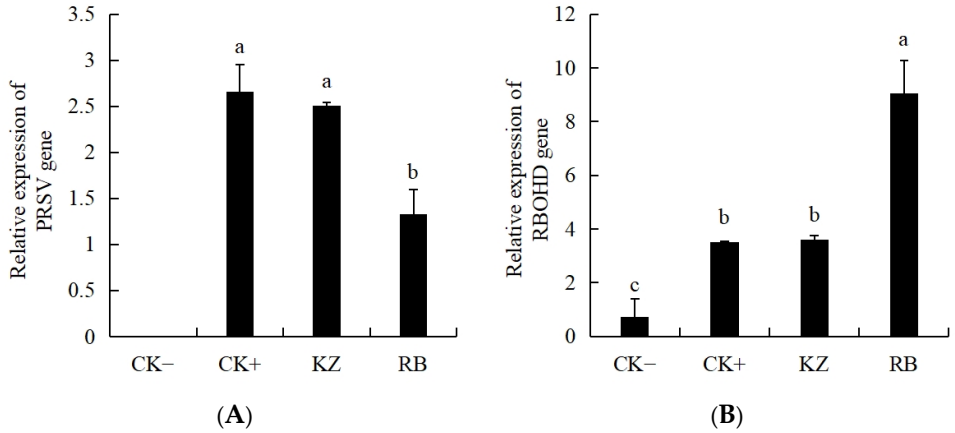


Figure 11. *CpRBOHD* gene transient expression verified by qPCR. Note: (**A**) and (**B**) show the expression of PRSV and *CpRBOHD* genes in different treatments, respectively. The treatments were as follows: plants that were not infected with PRSV and reconstructed overexpression vector were set as the negative control treatment (CK-); those infected with PRSV but not infected with reconstructed overexpression vector were set as the positive control treatment (CK+); those infected with PRSV and empty pCXSN vector were set as the control treatment (KZ); those infected with PRSV and reconstructed overexpression vector pCXSN-*CpRBOHD* were set as the RB treatment.

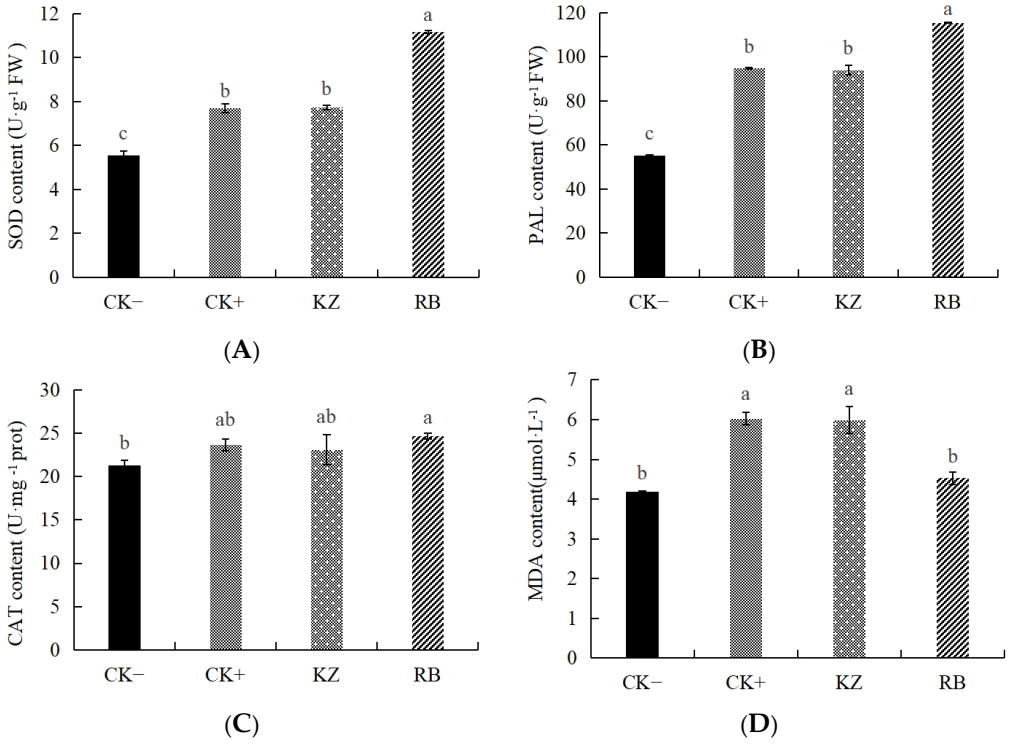
3.11.2. Analysis of Physiological Indices of Papaya Infected with CpRBOHD Gene

Superoxide dismutase (SOD) is a key plant antioxidant enzyme that catalyzes the disproportionation of superoxide radicals, scavenges superoxide anions, protects plant cells and tissues, and contributes to disease resistance [35]. Thus, SOD activity is positively correlated with plant antioxidant capacity. As shown in Figure 12A, SOD activity was ranked as RB (11.17) > CK+ (7.70) > KZ (7.72) > CK− (5.56). SOD activity in the RB treatment was significantly higher than that in the KZ, CK+, and CK− treatments. Specifically, the SOD activity in the RB treatment group was 45% higher than that in the infected positive control (CK+) group. Compared with the control group, the SOD activity in the RB treatment (achieved via transient expression) increased substantially ($p < 0.05$).

Phenylalanine ammonia lyase (PAL) is a key rate-limiting enzyme in the phenylpropanoid metabolic pathway that degrades harmful amines and synthesizes defense-related metabolites [36]. As shown in Figure 12B, PAL activity was ranked as RB (115.33) > CK+ (94.71) > KZ (94.00) > CK− (55.24). PAL activity in the RB treatment was significantly higher than that in CK− and CK+. Specifically, PAL in the RB treatment was 22% higher than that in the diseased CK+ ($p < 0.05$).

Catalase (CAT) is one of the most important antioxidant enzymes in plant cells. Appropriate levels of H_2O_2 can induce defense responses against oxidative stress [37], while excessive H_2O_2 causes peroxidative damage to cells; CAT mitigates this damage by catalyzing H_2O_2 decomposition. As shown in Figure 12C, CAT activity was ranked as RB (24.66) > CK+ (23.64) > KZ (23.10) > CK− (21.31). The CAT content in the RB treatment showed a significant difference compared to CK− ($p < 0.05$).

Under adverse conditions, plant cell membranes undergo lipid peroxidation, leading to increased membrane permeability and accumulation of malondialdehyde (MDA), an end product of lipid peroxidation [38]. MDA content reflects the degree of cell membrane damage and is negatively correlated with disease resistance [39]. As shown in Figure 12D. MDA content was ranked as CK+ (6.02) > KZ (5.99) > RB (4.53) > CK− (4.18). MDA content in the RB treatment was significantly lower than that in CK+ and KZ. Specifically, MDA content in the RB treatment was 25% lower than that in the infected positive CK+, indicating a significant reduction in MDA production ($p < 0.05$).



https://doi.org/10.3390/horticulturae12111373

Figure 12. Changes in physiological indices between different treatments. Note: (**A**): Changes in SOD between different treatments. (**B**): Changes in PAL between different treatments. (**C**): Changes in CAT between different treatments. (**D**): Changes in MDA between different treatments. The treatments were as follows: plants that were not infected with PRSV and reconstructed overexpression vector were set as the negative control treatment (CK-); those infected with PRSV but not infected with reconstructed overexpression vector were set as the positive control treatment (CK+); those infected with PRSV and empty pCXSN vector were set as the control treatment (KZ); those infected with PRSV and reconstructed overexpression vector pCXSN-*CpRBOHD* were set as the RB treatment.

4. Discussion

4.1. Changes in Antioxidant Enzymes and Related Hormones Against PRSV

When papaya is infected with PRSV, harmful metabolite accumulation increases and the activities of defense enzymes change. Pathogen infection typically induces significant upregulation of defense enzyme activities [38,40]. Under normal conditions, papaya exhibits higher disease resistance and lower levels of harmful metabolites. Our results show that the activities of PPO and SOD in all treatments were higher than those in CK, indicating that the application of CTS-N enhances papaya resistance to stress by increasing PPO and SOD activities. POD activity was positively correlated with plant disease resistance. POD activity in the CTS-N-treated plants was significantly higher than that in CK− and CK+, consistent with findings in cucumber [41]. Collectively, these results demonstrate that CTS-N treatment enhances papaya resistance to PRSV by suppressing viral replication and activating defense pathways. As a natural green immunomodulator, CTS-N can enhance the resistance of papaya to viral diseases, providing new insights for the management of PRSV. In the future, CTS-N is expected to help maintain papaya yield and quality while reducing production costs, thereby enhancing economic benefits.

Numerous studies have shown that both biotic and abiotic stresses induce the accumulation of ETH, JA, ABA, and SA, which enhance plant resistance [42,43]. Additionally, it could induce broad-spectrum resistance against pathogens including bacteria and viruses, and regulate plant growth. In our experiment, ETH content peaked within 24 h post-inoculation, particularly in Treatment B, consistent with findings by Wang and Yao [16]. JA levels also peaked in Treatment B after viral inoculation, aligning with results reported by He [44]. Chitinase activity followed the same trend as reported in pepper and cucumber [45]. CTS-N is a compound green control agent composed of multiple components, and it exhibits some control efficacy against PRSV. Researchers have found that either chitosan or metal ions alone in CTS-N can affect a plant's stress resistance process [8,10]. Subsequent experiments could evaluate the individual components of CTS-N for their respective resistance-inducing abilities against PRSV, thereby further elucidating the prevention and control capabilities of CTS-N components against this virus.

4.2. Cloning Analysis of CpRBOHD Gene from Papaya

KEGG pathway analysis of the aforementioned PRSV-resistant transcriptome induced by CTS-N revealed that *CpRBOHD* encodes an NADPH oxidase that generates ROS (Figure 13) [25]. Massive ROS production is a hallmark of the hypersensitive response (HR), which restricts viral spread [40]. Li et al. and Liu et al. reported that upregulated RBOH expression leads to ROS accumulation and enhanced disease resistance upon pathogen infection [46,47]. Transient expression assays in this study showed that elevated *CpRBOHD* expression in susceptible papaya leaves was associated with reduced PRSV levels. The qPCR-validated PRSV expression was consistent with findings by Huo [37].

qPCR further confirmed *CpRBOHD* upregulation; it was consistent with the research content reported by Huo et al. on the silencing of eIF4E [48], indicating that CpRBOHD is involved in PRSV resistance. Prokaryotic expression analysis confirmed that the selected hydrophilic fragment of *CpRBOHD* can be successfully expressed. This provides a basis for future studies on secondary metabolite changes during disease resistance at the protein level, as well as subsequent protein purification and in vitro functional analyses. Structurally, CpRBOHD possesses six transmembrane domains, which is consistent with previously reported RBOHs from other plant species [49].

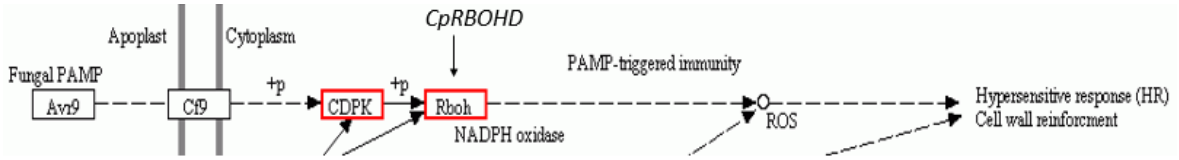


Figure 13. *CpRBOHD* participates in the conduction pathway (the transcriptome data of our previous experiments).

4.3. Superoxide Anion Changes and CpRBOHD Transient Expression

In this study, superoxide anion levels reflect the degree of membrane lipid peroxidation and the capacity of plants to scavenge excess ROS to minimize oxidative damage. It was found that CTS-N treatment effectively reduced superoxide anion content and enhanced defense enzyme activities in papaya. Additionally, it strengthened stress tolerance, mitigated oxidative damage, and slowed the progression of cellular injury in papaya. This result was consistent with previous findings by Li [46]. The level of reactive oxygen species was the lowest in Treatment B (Figure 6), and transient overexpression of *CpRBOHD* significantly increased the activities of the antioxidant enzymes SOD (Figure 12A) and CAT (Figure 12C), consistent with reports by Fan et al. [7]. RBOHD is an NADPH oxidase involved in ROS production. In subsequent experiments, by measuring ROS levels, we will verify that the upregulated expression of *CpRBOHD* promotes ROS generation, and that excessive ROS accumulation subsequently activates downstream antioxidant defense [50]. The upregulation of RBOHD triggers ROS burst, which subsequently activates the antioxidant system; this sequence of events is biologically plausible. However, the relationship among *CpRBOHD* expression, ROS production, and disease resistance warrants further investigation in subsequent experiments. Demonstrate the molecular mechanism by which *CpRBOHD* can mediate the defense response of ROS. Overexpression of *CpRBOHD* also increased PAL activity (Figure 12B), likely due to accelerated synthesis of PAL to degrade toxic amines produced during PRSV infection and reinforce plant defense. MDA content in the RB treatment was lower than that in CK+ and KZ (Figure 12D), indicating that *CpRBOHD* expression protects cell membrane integrity and reduces PRSV-induced cytopathic effects. In the transient expression experiments, the limited number of biological replicates precluded a more accurate elucidation of the defense mechanism mediated by *CpRBOHD* during PRSV infection in papaya leaves. The precise regulatory mechanisms underlying these observations warrant further investigation. This molecular mechanism can be further verified through methods such as *CpRBOHD* silencing or knockout, direct ROS measurements, detailed disease phenotyping following *CpRBOHD* manipulation.

In this study, we characterized the bioinformatics features of the papaya *CpRBOHD* gene, analyzed its expression dynamics during antiviral defense, and validated its prokaryotic expression, laying a foundation for further exploration of *CpRBOHD* functions and providing insights into the molecular regulation of *CpRBOHD*-mediated resistance to PRSV in papaya.

5. Conclusions

The application of 1.0 g/L CTS-N effectively enhanced papaya disease resistance, activated plant immune responses, suppressed PRSV invasion to a certain extent, and alleviated viral pathogenicity. The full-length *CpRBOHD* gene was cloned via RACE technology, and prokaryotic expression analysis confirmed that the selected hydrophilic fragment of *CpRBOHD* could be successfully expressed as a soluble protein. In transient expression assays of papaya leaves, the upregulation of *CpRBOHD* during PRSV infection triggered the activation of the plant's innate defense system, as evidenced by the increased activities of the antioxidant enzymes SOD, PAL, and CAT, alongside reduced MDA accumulation, ultimately enhancing papaya resistance against PRSV. This study demonstrates that *CpRBOHD* upregulation contributes to PRSV resistance in papaya at both physiological and molecular levels, laying a theoretical and practical foundation for dissecting the molecular mechanisms underlying *CpRBOHD*-mediated antiviral defense and providing a promising strategy for sustainable disease management and yield protection in papaya cultivation.

Supplementary Materials: The following supporting information can be downloaded at: https://www.mdpi.com/article/10.3390/horticulturae12111373/s1, Figure S1: *CpRBOHD* PCR clone electropherogram; Figure S2: Prediction of signal peptide of CpRBOHD protein; Figure S3: Prediction of transmembrane domains of CpRBOHD protein; Figure S4: RNA gel image; Figure S5: Identification of recombinant expression vector pET28a-*CpRBOHD*-sumo; Table S1: Summary of Primers Used(5′- 3′); Table S2: 20uL Reverse transcriptase system; Table S3: 20uL PCR reaction system; Table S4: 20uL qPCR reaction system; Table S5: Bioinformatics Analysis Online Software.

Author Contributions: P.C. provided experimental ideas and supervised and guided the whole experiment. J.L. and N.A. conducted the experiment and drafted the manuscript. J.L., N.A., Y.G. and P.C. analyzed data and revised the manuscript. All authors have read and agreed to the published version of the manuscript.

Funding: This research was funded by the Hainan Provincial Natural Science Foundation of China (grant number: 320RC491).

Data Availability Statement: The raw data supporting the conclusions of this article will be made available by the authors on request.

Conflicts of Interest: The authors declare no conflicts of interest.

References

1. Zhou, Z.; Ford, R.; Bar, I.; Kanchana-Udomkan, C. Papaya (*Carica papaya* L.) Flavour Profiling. *Genes* **2021**, *12*, 1416.
2. Zhang, R.P.; Fan, J.H.; Chen, H.J.; Yan, X.X.; Chen, P. Study on the control effect of three biological pesticides on papaya ring spot virus. *South China Fruits* **2017**, *46*, 79–82.
3. Tuo, D.C. Construction and Infectivity Assays of Full-Length cDNA Clones of Papaya Ringspot Virus Type P in HaiNan (PRSV-P HN-2). Master's Thesis, Hainan University, Haikou, China, 2011.
4. Jyotika, R.K.; Harish, S.; Karthikeyan, G.; Kumar, K.K.; Murugan, M.; Jayakanthan, M.; Chen, T.C. Molecular approaches for the management of papaya ringspot virus infecting papaya: A comprehensive review. *Mol. Biol. Rep.* **2026**, *51*, 981.
5. Saleem, A.; Ali, Z.; Yeh, S.-D.; Saeed, W.; Binat Imdad, A.; Akbar, M.F.; Goodman, R.E.; Naseem, S. Genetic variability and evolutionary dynamics of atypical Papaya ringspot virus infecting Papaya. *PLoS ONE* **2021**, *16*, e0258298.
6. Gao, W. Applications of Chitin and Chitosan in Agriculture. *Agric. Technol.* **2005**, *25*, 84–85.
7. Fan, H.; Yan, X.; Fu, M.; Liu, D.; Awan, A.W.; Chen, P.; Rasheed, S.M.; Gao, L.; Zhang, R. Interactive Effect of Biological Agents Chitosan, Lentinan and Ningnanmycin on Papaya Ringspot Virus Resistance in Papaya (*Carica papaya* L.). *Molecules* **2022**, *27*, 7474.
8. Zhang, X.Q.; Zheng, M.Q.; Lai, R.Y.; Zhong, Z.H. Control efficiency of inducers to Papaya ringspot virus disease in *Carica papaya*. *Plant Prot.* **2012**, *38*, 178–181.

9. Liu, Z.H.; Chen, S.; Le, X.Y. Effects of Chitosan Supported Cu (II), Mn(II) Complexes on Seed Germination and Salt-tolerance of Seedling Growth of Maize. *Chin. Agric. Sci. Bull.* **2010**, *26*, 169–173.
10. Liu, Z.H.; Li, Y.J.; Le, X.Y.; Chen, S. Effects of Chitosan supported Fe(II), Zn(II) complexes on seed germination and salt-tolerance of seedling growth of Maize. *Guangdong Agric. Sci.* **2010**, *37*, 12–14.
11. Prashanth, K.V.H.; Dharmesh, S.M.; Rao, K.S.J.; Tharanathan, R.N. Free radical-induced chitosan depolymerized products protect calf thymus DNA from oxidative damage. *Carbohydr. Res.* **2007**, *342*, 190–195.
12. Collinge, D.B.; Kragh, K.M.; Mikkelsen, J.D.; Nielsen, K.K.; Rasmussen, U.; Vad, K. Plant chitinases. *Plant J.* **1993**, *3*, 31–40.
13. Kumar, A.; Basavaraj, Y.B.; Kumar, P.; Yadav, M.K.; Singh, S.K. Development of transgene construct using coat protein gene of papaya ringspot virus and its validation. *Progress. Agric.* **2018**, *18*, 92–97.
14. Jia, R.; Zhao, H.; Huang, J.; Kong, H.; Zhang, Y.; Guo, J.; Huang, Q.; Guo, Y.; Wei, Q.; Zuo, J.; et al. Publisher Correction: Use of RNAi technology to develop a PRSV-resistant transgenic papaya. *Sci. Rep.* **2017**, *7*, 16390.
15. Oda, T.; Hashimoto, H.; Kuwabara, N.; Akashi, S.; Hayashi, K.; Kojima, C.; Wong, H.L.; Kawasaki, T.; Shimamoto, K.; Sato, M.; et al. Structure of the N-terminal regulatory domain of a plant NADPH oxidase and its functional implications. *J. Biol. Chem.* **2009**, *285*, 1435–1445.
16. Wang, Z.; Yao, Y.A. Jasmonic acid and ethylene signaling pathways are involved in defense responses against Sclerotinia sclerotiorum in oilseed rape. *J. Biol.* **2013**, *30*, 1–4+13.
17. Torres, M.A.; Jones, J.D.; Dang, J.L. Reactive oxygen species signaling in response to pathogens. *Plant Physiol.* **2006**, *1411*, 373–378.
18. Lu, X. *NbRbohB* is Required for Resistance to Phytophthora Pathogens in *Nicotiana benthamiana*. *J. Plant Prot.* **2014**, *41*, 622–629.
19. Castro, B.; Citterico, M.; Kimura, S.; Stevens, D.M.; Wrzaczek, M.; Coaker, G. Stress-induced reactive oxygen species compartmentalization, perception and signalling. *Nat. Plants* **2021**, *7*, 403–412.
20. Kora, D.; Bhattacharjee, S. The interaction of reactive oxygen species and antioxidants at the metabolic interface in salicylic acid-induced adventitious root formation in mung bean [*Vigna radiata* (L.) R. Wilczek]. *J. Plant Physiol.* **2020**, *248*, 153152.
21. Qi, X.; Li, Q.; Ma, X.; Qian, C.; Wang, H.; Ren, N.; Shen, C.; Huang, S.; Xu, X.; Xu, Q.; et al. Waterlogging-induced adventitious root formation in cucumber is regulated by ethylene and auxin through reactive oxygen species signalling. *Plant Cell Environ.* **2019**, *42*, 1458–1470.
22. Huang, A.; Wang, Y.; Liu, Y.; Wang, G.; She, X. Reactive oxygen species regulate auxin levels to mediate adventitious root induction in *Arabidopsis hypocotyl* cuttings. *J. Integr. Plant Biol.* **2020**, *62*, 912–926.
23. Zhang, Y.; Yang, X.; Nvsvrot, T.; Huang, L.; Cai, G.; Ding, Y.; Ren, W.; Wang, N. The transcription factor *WRKY75* regulates the development of adventitious roots, lateral buds and callus by modulating hydrogen peroxide content in poplar. *J. Exp. Bot.* **2022**, *73*, 1483–1498.
24. Cheng, C.; Che, Q.; Su, S.; Liu, Y.; Wang, Y.; Xu, X. Genome-wide identification and characterization of Respiratory Burst Oxidase Homolog genes in six Rosaceae species and an analysis of their effects on adventitious rooting in apple. *PLoS ONE* **2020**, *15*, e0239705.
25. An, N.; Lv, J.-H.; Ma, H.-Q.; Chen, P.; Cao, H.; Martin, J.J.J. Transcript Profiling of Papaya (*Carica papaya* L.) with CTS-N Fertiliser after Inoculation with PRSV. *J. Hortic. Sci. Biotechnol.* **2022**, *97*, 466–475.
26. Chen, L. *Tutorials of Biological Electron Microscopy*; Beijing Normal University Press: Beijing, China, 1998.
27. Wang, X.K. *Principles and Techniques of Plant Physiology and Biochemistry Experiments*, 2nd ed.; Higher Education Press: Beijing, China, 2006.
28. Tang, Z.C. *Modern Guide to Plant Physiology Experiments*; Science Press: Beijing, China, 1999.
29. Li, G.Z.; Gong, M. Improvement of the Method for Measuring the Activity of Plant Polyphenol Oxidase. *J. Yunnan Norm. Univ. Nat. Sci. Edition.* **2005**, *25*, 44–45.
30. Li, G.Z.; Gong, M. Improvement of the Method for Measuring Superoxide Anion Free Radicals in Plants. *Yunnan Bot. Res.* **2005**, *27*, 211–216.
31. Chen, P.; Liu, Q.Z. Effects of *Tetranychus urticae* feeding on the H_2O_2, MDA content and some defensive enzyme activities in strawberry leaves. *J. Environ. Entomol.* **2022**, *44*, 697–703.
32. Liu, Z.; Ouyang, Y.; Gong, J.; Zheng, X. Electron microscopic observation and purification of PRSV. *Trop. Agric. Sci.* **1992**, 12, 45–47+38.
33. Sun, J.; Li, F.; Wang, Y.; Wang, H.; Wang, C.; Chen, H. Pathogen Identification of the Mosaic Disease of Papaya in Yunnan. *J. Yunnan Agric. Univ.* **2006**, *21*, 838–841.

34. He, H. Study on Effects of ABA on Stress Resistance and Fruit Quality of Grape. Master's Thesis, Sichuan Agricultural University, Chengdu, China, 2013.
35. Xia, M.; Wang, W.; Yuan, R.; Deng, F.; Shen, F. Superoxide Dismutase and Its Research in Plant Stress-tolerance. *Mol. Plant Breed.* **2015**, *13*, 2633–2646.
36. Vogt, T. Phenylpropanoid Biosynthesis. *Mol. Plant* **2010**, *3*, 2–20.
37. Li, H.; Liu, D.; He, H.; Zhang, N.; Ge, F.; Chen, Z. The Role of Germin-Like Protein in Plant Defense Responses. *Plant Physiol. J.* **2013**, *49*, 331–336.
38. Wu, M.L.; Li, P.; Yu, W.G.; Huang, W.H.; Xiong, J.S.; Liu, W.Z.; Fang, Z.J.; Xu, N.; Wang, W.J. Advances in the Research of Relationship between Defensive Enzymes and Disease Resistance in Rice. *Mol. Plant Breed.* **2024**, *22*, 2413–2420.
39. Cui, Y. Study on Two Kinds of Crassulaceae Plant Resistance. Master's Thesis, Central South University of Forestry and Technology, Changsha, China, 2014.
40. Zhang, B.; Pan, C.; Feng, C.; Yan, C.; Yu, Y.; Chen, Z.; Guo, C.; Wang, X. Role of mitochondrial reactive oxygen species in homeostasis regulation. *Redox Rep. Commun. Free Radic. Res.* **2022**, *27*, 45–52.
41. Yu, Y.; Schjoerring, J.K.; Du, X. Effects of silicon on the activities of defense-related enzymes in cucumber inoculated with *Pseudoperonospora cubensis*. *J. Plant Nutr.* **2011**, *34*, 243–257.
42. Verma, V.; Ravindran, P.; Kumar, P.P. Plant hormone-mediated regulation of stress responses. *BMC Plant Biol.* **2016**, *16*, 86.
43. Feng, Y.; Li, Z.; Kong, X.; Khan, A.; Ullah, N.; Zhang, X. Plant Coping with Cold Stress: Molecular and Physiological Adaptive Mechanisms with Future Perspectives. *Cells* **2025**, *14*, 110.
44. He, Y. Jasmonic Acid-Mediated Defense Suppresses Brassinosteroid-Mediated Susceptibility to Rice Black Streaked Dwarf Virus Infection in rice. Ph.D. thesis, Zhejiang University, Hangzhou, China, 2017.
45. Sang, M.K.; Kim, K.D. Biocontrol activity and primed systemic resistance by compost water extracts against anthracnoses of pepper and cucumber. *Phytopathology* **2011**, *101*, 732–740.
46. Li, G. Study on the production of superoxide anion and its function in plants. *Biotechnol. World* **2012**, *10*, 24–25.
47. Liu, Q.; He, H.; Hu, L. Research Progress in Plant Rboh Genes Function and Activity Regulation Mechanism. *Biotechnol. Bull.* **2013**, 8–13.
48. Huo, P. Papaya Viruses Identification Using Multiplex Real-Time RT-PCR and The Interference Effect Research of Papaya *eIF4E* Family Genes. Master's Thesis, Hainan University, Haikou, China, 2015.
49. Ogasawara, Y.; Kaya, H.; Hiraoka, G.; Yumoto, F.; Kimura, S.; Kadota, Y.; Hishinuma, H.; Senzaki, E.; Yamagoe, S.; Nagata, K.; et al. Synergistic activation of the *Arabidopsis* NADPH oxidase atrbohd by Ca^{2+} and phosphorylation. *J. Biol. Chem.* **2008**, *283*, 8885–8892.
50. Bedard, K.; Lardy, B.; Krause, K.-H. NOX family NADPH oxidases: Not just in mammals. *Biochimie* **2007**, *89*, 1107–1112.

Disclaimer/Publisher's Note: The statements, opinions and data contained in all publications are solely those of the individual author(s) and contributor(s) and not of MDPI and/or the editor(s). MDPI and/or the editor(s) disclaim responsibility for any injury to people or property resulting from any ideas, methods, instructions or products referred to in the content.